Journal of Alloys and Compounds 729 (2017) 648–654

Contents lists available at ScienceDirect

Journal of Alloys and Compounds

journal homepage: http://www.elsevier.com/locate/jalcom

Preparations and de/re-hydrogenation properties of $Li_xNa_{3-x}AlH_6$ (x=0.9–1.3) non-stoichiometric compounds

Xiaolu Fan [a], Yao Zhang [a, c, *], Yunfeng Zhu [b, c, **], Cassandra Phillips [d], Xinli Guo [a], Jian Chen [a], Zengmei Wang [a], Liquan Li [b, c]

[a] School of Materials Science and Engineering, Jiangsu Key Laboratory of Advanced Metallic Materials, Southeast University, Nanjing 211189, China
[b] College of Materials Science and Engineering, Nanjing Tech University, 5 Xinmofan Road, Nanjing 210009, China
[c] Jiangsu Collaborative Innovation Center for Advanced Inorganic Function Composites, Nanjing Tech University, Nanjing 210009, China
[d] Department of Physics and Astronomy, Washington State University, Pullman, WA 99163, USA

ARTICLE INFO

Article history:
Received 27 June 2017
Received in revised form
18 September 2017
Accepted 19 September 2017
Available online 21 September 2017

Keywords:
Mixed alkali metals alanates
Hydrogen storage performances
Thermal stability
Kinetics

ABSTRACT

Mixed alkali alanates $Li_xNa_{3-x}AlH_6$ have been successfully synthesized by means of grinding mixtures of Li_3AlH_6 and Na_3AlH_6 in specific molar ratios. Non-stoichiometric $Li_xNa_{3-x}AlH_6$ compounds with single perovskite-type structures (space group Fm-3m) can be formed only within the composition range of x = 0.9–1.3. $Li_{1.3}Na_{1.7}AlH_6$ exhibits superior hydrogen storage properties over other $Li_xNa_{3-x}AlH_6$ compounds. Its onset dehydrogenation temperature (~423 K) was lowered by more than 40 K from other samples in temperature programmed dehydrogenation (TPD) curves. Also, the dehydrogenation capacity of $Li_{1.3}Na_{1.7}AlH_6$ (3.45 wt.%) is the highest among the compounds. The dehydrogenation enthalpy values of $Li_xNa_{3-x}AlH_6$ decreased as x increased from 0.9 to 1.3 according to the results by isothermal pressure-composition (PCI) curves and van't Hoff plots. It shows that the dehydrogenation $Li_{1.3}Na_{1.7}AlH_6$ (49.7 kJ mol H_2^{-1}) was greatly destabilized from that of $LiNa_2AlH_6$ (68.1 kJ mol H_2^{-1}). Furthermore, the apparent activation energy of dehydrogenation for $Li_{1.3}Na_{1.7}AlH_6$ (138.1 kJ mol^{-1}) was remarkably lowered from that of $LiNa_2AlH_6$. This illustrates that $Li_{1.3}Na_{1.7}AlH_6$ exhibits enhanced dehydrogenation kinetics from that of $LiNa_2AlH_6$.

1. Introduction

As well known, hydrogen is very important as a new source of renewable energy [1]. However, the emerged hydrogen storage materials cannot fully meet the standards of utilizations [2]. Some complex hydrides, such as $NaAlH_4$, potentially reach the target of both gravimetric and volumetric densities [3–11]. It's possible for the de/re-hydrogenation capacity of $NaAlH_4$ to attain more than 4.5 wt.% H_2 at a temperature below 473 K using Ti-based additives [12–16]. In recent years, studies have been expanded to include mixed alkali alanates such as $LiNa_2AlH_6$, LiK_2AlH_6, and K_2NaAlH_6 etc. People have already synthesized these materials and investigated their hydrogen storage performances extensively [17–32].

Among these compounds, $LiNa_2AlH_6$ exhibits a large dehydrogenation capacity. Approximately 6.7 wt.% H_2 can be evolved from the compound through a three-step reaction within the temperature range from 463 K to 753 K [31]. Many methods to synthesize $LiNa_2AlH_6$ have been developed during the last decades. Wang et al. obtained $LiNa_2AlH_6$ by solid-state reaction among LiH, NaH, and $NaAlH_4$ at a ratio of 1:1:1. Nearly 3.35 wt.% H_2 can be released during the first stage of dehydrogenation [31,32]. Claudy et al. [17] combined $LiAlH_4$ with NaH to achieve $LiNa_2AlH_6$ via either toluene or a solid-state reaction at high temperatures and under high hydrogen pressures. Huot et al. [20] obtained $LiNa_2AlH_6$ by means of mechanochemical method without any solvent, which supplied a facile way to yield the product. Since then, the ball milling method has been extensively used in many combinations such as 2NaH-$LiAlH_4$ [26,27], NaH-$LiAlH_4$ [23], 2$NaAlH_4$-LiH [22], and $NaAlH_4$-NaH-LiH [25] for synthesizing $LiNa_2AlH_6$.

* Corresponding author. School of Materials Science and Engineering, Jiangsu Key Laboratory of Advanced Metallic Materials, Southeast University, Nanjing 211189, China.
** Corresponding author. College of Materials Science and Engineering, Nanjing Tech University, 5 Xinmofan Road, Nanjing 210009, China.
E-mail addresses: zhangyao@seu.edu.cn (Y. Zhang), yfzhu@njtech.edu.cn (Y. Zhu).

https://doi.org/10.1016/j.jallcom.2017.09.205
0925-8388/

Some other works were conducted to adjust the atomic ratio of Li to Na of the $LiNa_2AlH_6$ phase in order to optimize its thermal stability and dehydrogenation performances. However, only a few compounds have been achieved up to date [33,34]. The composition range of x in $Li_xNa_{3-x}AlH_6$ compounds is still imprecise. The effects of x on the structures and thermal stabilities of these compounds are also unknown.

In the present work, we explored different values of x for $Li_xNa_{3-x}AlH_6$ and the hydrogen storage performances for each. X-ray diffraction (XRD) measurements were implemented to characterize the structures of these compounds. Differential scanning calorimeter (DSC), temperature programmed dehydrogenation (TPD), and pressure-composition isotherms (PCI) measurements were carried out to study the dehydrogenation properties of these samples. We primarily found that x = 1.3 exhibits the best thermodynamic and kinetic properties from the x values that we studied.

2. Experimental

Chemicals NaH (95%, Sigma–Aldrich), $NaAlH_4$ (93%, Sigma–Aldrich), LiH (97%, Aladdin), and $LiAlH_4$ (97%, Alfa Aesar) were all used without pretreatment. Na_3AlH_6 was synthesized by ball milling NaH and $NaAlH_4$ in the molar ratio of 2:1 for 20 h under high-purity (99.9999%) argon on a planetary ball mill (QM-3SP4, Nanjing) at 500 rpm. Li_3AlH_6 was synthesized by ball milling LiH and $LiAlH_4$ in the molar ratio of 2:1 for 5 h under high-purity (99.9999%) argon at 450 rpm. The mixtures Li_3AlH_6 and Na_3AlH_6 were milled in specific molar ratios for 10 h to form Li-Na-Al-H compounds at a rotation rate of 500 rpm. The ball-to-powder weight ratio was about 65:1.

Both PCI and TPD measurements were carried out on a home-made Sieverts-type apparatus [35,36]. A sample tested by DSC (TA Q2000) was about 5 mg and used carrier gas of 0.1 MPa Ar with a purge rate of 50 ml min^{-1}. All the measurements were performed at a ramping rate of 5 k min^{-1}.

Structural characteristics of the samples were conducted by powder X-ray diffraction (XRD, X'Pert PRO of PANalytical) with Cu-Ka radiation at 40 kV and 40 mA. The diffraction degree (2θ) was scanned from 10° to 90° with a step width of 0.02. All handlings on the samples were performed in glove box full of high-purity Ar (99.9999%). A cellophane tape was placed on the sample pool to protect the sample from the air and moisture during XRD measurement.

3. Results and discussion

3.1. Structures of mixed alkali metal alanates

The $Li_xNa_{3-x}AlH_6$ compounds were synthesized by ball milling the mixtures of Li_3AlH_6 and Na_3AlH_6 at different ratios (x = 0.9–1.3). The reaction was expressed by equation (1).

$$xLi_3AlH_6 + (3\text{-}x)\ Na_3AlH_6 \rightarrow 3Li_xNa_{3-x}AlH_6 \quad (1)$$

Single phase Li-Na-Al-H (S.G. Fm-3m) can be identified only within the composition range of x = 0.9–1.3 as shown in the XRD patterns of Fig. 1a and b. When x is lower than 0.9, Na_3AlH_6 appears in the XRD pattern. When x exceeds 1.4, an unknown phase could be formed. The lattice parameters were evaluated by using Jade software [37] and are summarized in Fig. 1c. It was found that these lattice parameters continuously decrease with the augmentation of x from 0.9 to 1.3. Fig. S1 exhibits the Rietveld refinements results in the XRD patterns of $Li_xNa_{(3-x)}AlH_6$ (x = 0.9–1.3). The refinements

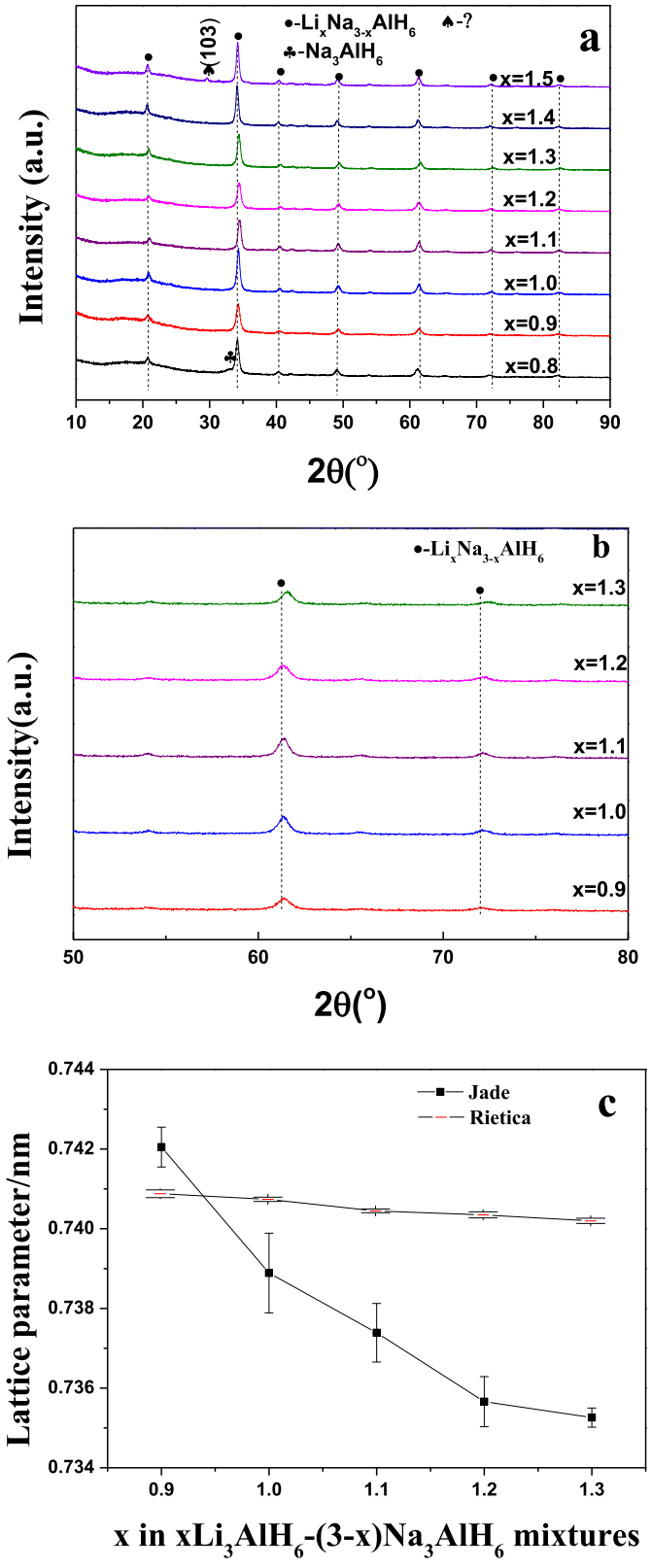

Fig. 1. a) XRD patterns of xLi_3AlH_6–$(3\text{-}x)Na_3AlH_6$ system synthesized by ball milling (x = 0.8–1.5); b) XRD patterns of xLi_3AlH_6–$(3\text{-}x)Na_3AlH_6$ within the Bragg angle ranging from 50° to 80° (x = 0.9–1.3); c) Dependencies of the lattice parameters upon x value by means of Jade and Rietica (Rietveld refinement) software, respectively.

results demonstrated the continuous variation of lattice parameter with increasing x amount, which agrees well with those obtained by Jade as shown in Fig. 1c. However, the atomic coordinates of Li, Na, Al, and H in the perovskite-type structure (Fm-3m) phase are hardly observed in the present work. Further efforts on $Li_xNa_{3-x}AlD_6$ by means of synchrotron X-ray diffraction analyses are ongoing.

Calculation methods by Jade and Rietica are thoroughly different. Rietica method determining results of lattice parameters is mainly based on the Rietveld refinements on XRD patterns. However, the Jade method determined lattice parameters and crystalline sizes mainly on the basis of the Bragg angles and the FWHM of diffraction peaks, respectively. Both methods are thoroughly different. However, dependencies of lattice parameters upon x values are nearly the same for both methods. It suggests that variations of lattice parameters are double checked and demonstrated.

3.2. De/re-hydrogenation properties of $Li_xNa_{3-x}AlH_6$

The temperature programmed desorption curves of $Li_xNa_{3-x}AlH_6$ (x = 0.9–1.3) exhibited in Fig. 2 indicate that, with the increase of x, the dehydrogenation capacity gradually increases. This phenomenon can be ascribed to the increased amount of lightweight lithium in the compounds. When x amount of Li is gradually increased from 0.9 to 1.3, the onset temperatures of dehydrogenation lowers accordingly. Furthermore, when x reaches 1.3, its onset temperature is reduced to 423 K, which is lower than other samples by at least 40 K. Also, the dehydrogenation capacity of the compound reaches 3.45 wt.% H_2, which is the highest capacity among these single phase Li-Na-Al-H compounds.

Fig. 3 a shows the XRD patterns of $Li_xNa_{3-x}AlH_6$ (x = 0.9–1.3) compounds annealed at 573 K. The identified LiH, NaH, and Al phases imply that these compounds went through the same desorption process, which can be expressed as follows.

$$Li_xNa_{3-x}AlH_6 \rightarrow xLiH + (3-x)NaH + Al + 3/2H_2 \quad (2)$$

Fig. 3b shows the XRD patterns of $Li_{1.3}Na_{1.7}AlH_6$ annealed at temperature 453 K, 483 K, 503 K and 523 K, respectively. Those identified phases suggest that the reaction pathway of $Li_{1.3}Na_{1.7}AlH_6$ is the same as the other $Li_xNa_{3-x}AlH_6$ samples as equation (2).

Fig. 4 describes the hydrogenation performances for as-dehydrogenated $Li_xNa_{3-x}AlH_6$ compounds. It reveals that the duration time until saturated hydrogenation gradually decreased with an increase of x in $Li_xNa_{3-x}AlH_6$. Among these samples, $Li_{1.3}Na_{1.7}AlH_6$ exhibits the shortest saturation time and the highest isothermal hydrogenation rate. In XRD patterns of Fig. 5, there is still some NaH, LiH, and Al phases and has a perovskite-type structure. It means that the reaction was not completed. Both kinetic and thermodynamic barriers likely hindered its rehydrogenation.

3.3. De/re-hydrogenation kinetics of $Li_xNa_{3-x}AlH_6$

Fig. 6 (a), (b), and (c) present the DSC curves measured at different ramping rates for $LiNa_2AlH_6$, $Li_{1.2}Na_{1.8}AlH_6$ and $Li_{1.3}Na_{1.7}AlH_6$, respectively. Based on these curves, the activation energy values of desorption from these samples can be determined

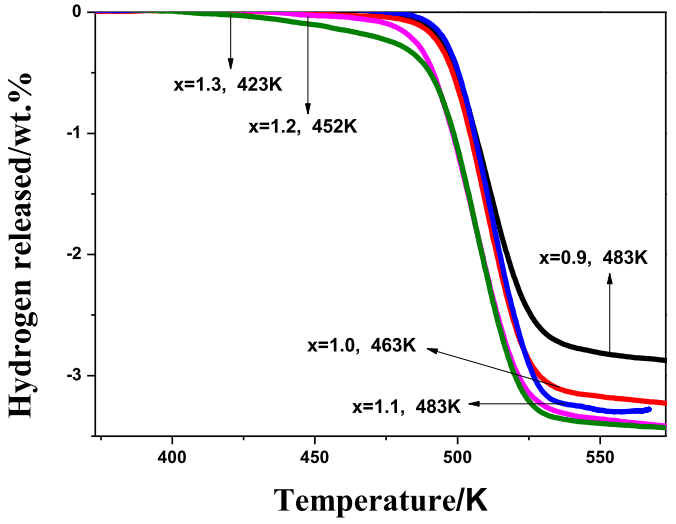

Fig. 2. Temperature programmed desorption (TPD) curves of $Li_xNa_{3-x}AlH_6$ compounds synthesized by ball milling.

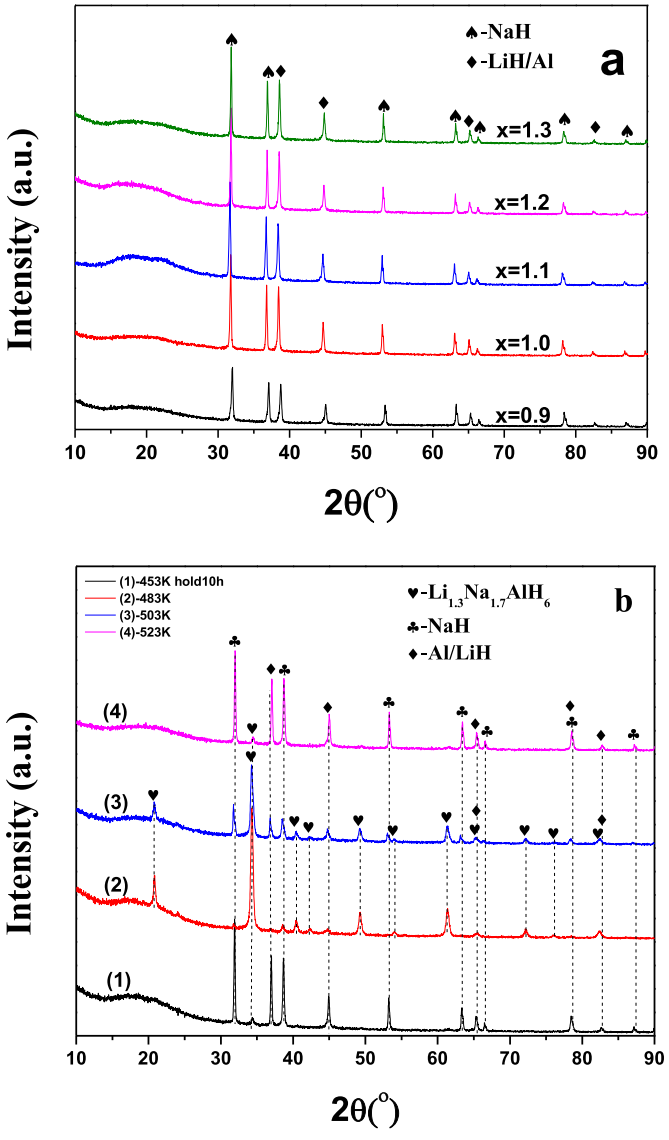

Fig. 3. a) XRD patterns of $Li_xNa_{3-x}AlH_6$ samples as annealed at 573 K; b) XRD pattern of $Li_{1.3}Na_{1.7}AlH_6$ sample as annealed at 453 K for 10hr, 483 K, 503 K, and 523 K, respectively.

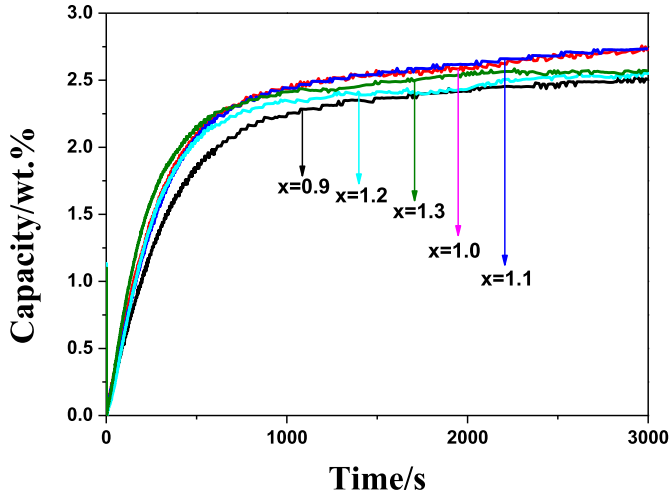

Fig. 4. Isothermal hydrogenation curves of the Li-Na-Al-H samples at 507 K and under hydrogen pressure of 5 MPa.

by means of Kissinger's equation (3).

$$\ln\left(\frac{\beta}{T_p^2}\right) = -\frac{E_a}{R}\cdot\frac{1}{T_p} + C \tag{3}$$

In this equation, β is the ramping rate, T_p stands for the peak temperature, and R represents the gas constant.

The apparent activation energy E_a for dehydrogenation of $LiNa_2AlH_6$ is 162 kJ mol^{-1} which approaches the value of previous work (173 kJ mol^{-1}) [32]. It was found that with an increase of x in $Li_xNa_{3-x}AlH_6$, the E_a value would be gradually reduced. It means that the dehydrogenation kinetic barrier was weakened with the increase of the Li amount in the compound. Therefore, the dehydrogenation kinetics and reaction rate were enhanced. According to the results summarized in Table 1, $Li_{1.3}Na_{1.7}AlH_6$ offers the lowest apparent activation energy (138.1 kJ mol^{-1}) among these compounds, which enhances its dehydrogenation kinetics.

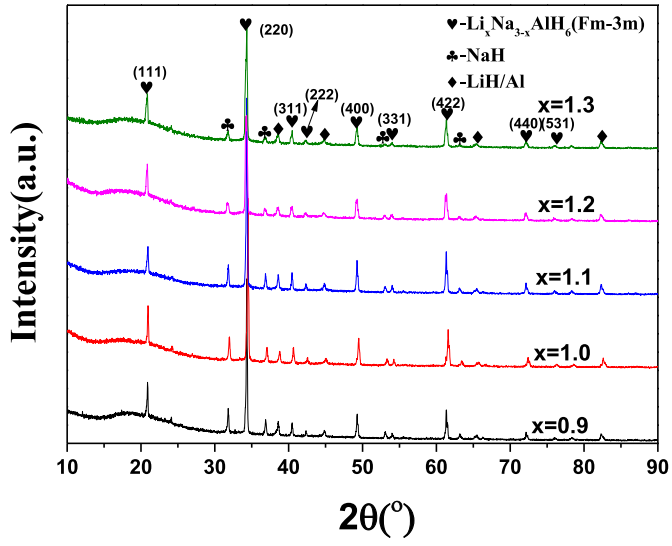

Fig. 5. XRD patterns of those $Li_xNa_{3-x}AlH_6$ (x = 0.9–1.3) samples after isothermal hydrogenation.

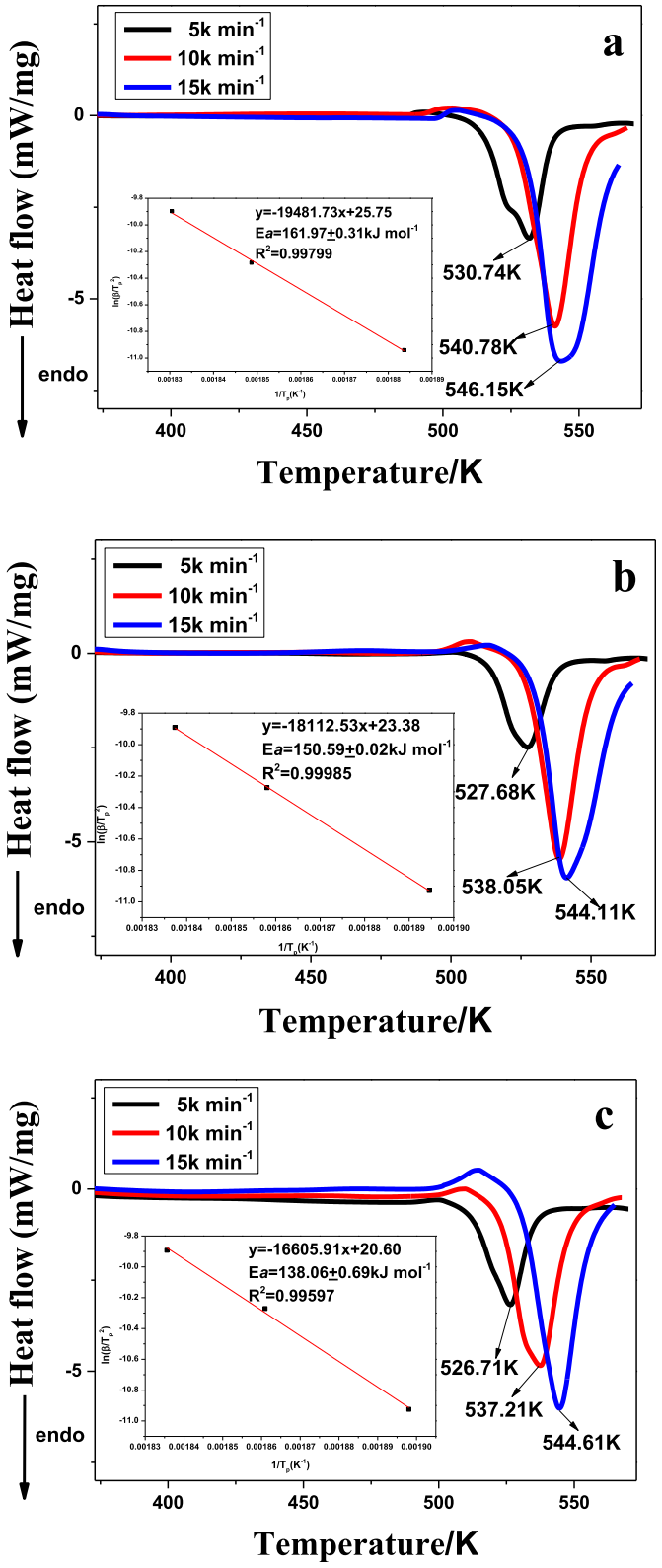

Fig. 6. a) DSC curves of $LiNa_2AlH_6$ measured at rates of 5 k min^{-1}, 10 k min^{-1} and 15 k min^{-1}, respectively; b) DSC curves of $Li_{1.2}Na_{1.8}AlH_6$ measured at rates of 5 k min^{-1}, 10 k min^{-1} and 15 k min^{-1}, respectively; c) DSC curves of $Li_{1.3}Na_{1.7}AlH_6$ measured at rates of 5 k min^{-1}, 10 k min^{-1} and 15 k min^{-1}, respectively. Figure's insets present those fitted plots to evaluate their activation energies of dehydrogenations by means of Kissinger's method.

Fig. 7(a), (b), and (c) reflect the isothermal rehydrogenation behaviors of $LiNa_2AlH_6$, $Li_{1.2}Na_{1.8}AlH_6$ and $Li_{1.3}Na_{1.7}AlH_6$ compounds tested at different temperatures. Their absorption activation energies were identified by the Arrhenius formula as equation (4) and the Johnson-Mehl-Avrami (JMA) equation (5) [26].

$$\ln k = -\frac{E_a}{RT} + \ln A \tag{4}$$

$$\alpha = 1 - e^{-(kt)^n} \tag{5}$$

Where k represents the reaction rate constant, E_a stands for the hydrogen absorption activation energy, T is temperature, R belongs to the gas constant, A is assigned as pre-exponential factor, and α is a constant.

According to the results summarized in Table 1, those hydrogenation activation energy values are very close to these compounds, which means that increasing the Li amount in Li-Na-Al-H compounds would slightly improve the kinetics of hydrogenation.

3.4. Thermal stabilities of $Li_xNa_{3-x}AlH_6$

The dehydrogenation enthalpies ΔH were employed to represent the thermal stabilities of $Li_xNa_{3-x}AlH_6$. In order to reveal the effects of x on their thermal stabilities, these ΔH values were investigated by means of PCI curves in Fig. 8 and their van't Hoff equation (6) as follows.

$$\ln P = \frac{1}{T}\left(\frac{-\Delta H}{R}\right) + C \tag{6}$$

P is the plateau pressure, T is the temperature, ΔH is the desorption enthalpy, and R is the gas constant.

As shown in Table 2, the enthalpy value of $LiNa_2AlH_6$ (68.1 kJ mol H_2^{-1}) is close to the value of previous work (63 kJ mol H_2^{-1}) [31,32]. Here, those ΔH values of $Li_xNa_{3-x}AlH_6$ compounds were remarkably reduced with increasing x in these compounds. $Li_{1.3}Na_{1.7}AlH_6$ possesses the lowest dehydrogenation enthalpy value (49.7 kJ mol H_2^{-1}) among these Li-Na-Al-H compounds. The enthalpy value of $Li_{1.3}Na_{1.7}AlH_6$ closes to that of Na_3AlH_6 (47 kJ mol H_2^{-1}) [3] but is higher than that of Li_3AlH_6 (15 kJ mol H_2^{-1}) [38]. Furthermore, all PCI curves possessing one plateau demonstrate again that each sample of $Li_xNa_{3-x}AlH_6$ only has a single phase.

$Li_{1.3}Na_{1.7}AlH_6$ is the most destabilized sample, which should be beneficial to reducing its onset dehydrogenation temperature as shown in Fig. 2. Therefore, it can be concluded that $Li_{1.3}Na_{1.7}AlH_6$ is the optimized species among all Li-Na-Al-H compounds due to its superior thermal stability and activation energy.

4. Conclusion

1) In the present work, non-stoichiometric $Li_xNa_{3-x}AlH_6$ compounds were successfully synthesized through ball milling the mixtures of Li_3AlH_6 with Na_3AlH_6 in specific molecular ratios.

Table 1
Desorption and absorption activation energies of $Li_xNa_{3-x}AlH_6$ compounds.

Compound	$LiNa_2AlH_6$	$Li_{1.2}Na_{1.8}AlH_6$	$Li_{1.3}Na_{1.7}AlH_6$
E_a (KJ mol^{-1}) of dehydrogenation	162.0	150.6	138.1
E_a (KJ mol^{-1}) of rehydrognation	63.2	53.6	59.8

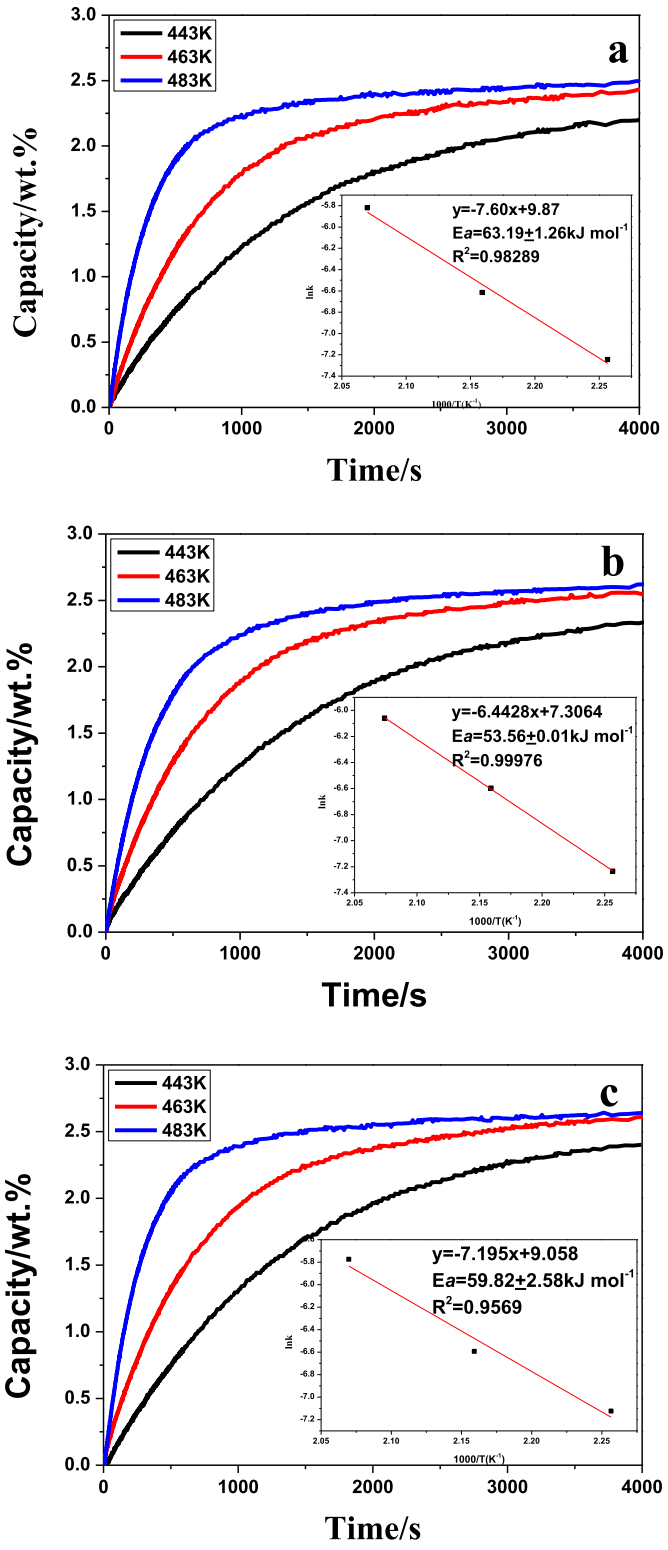

Fig. 7. a) Isothermal hydrogenation curves of $LiNa_2AlH_6$ obtained at temperatures of 443 K, 463 K, and 483 K, respectively; b) Isothermal hydrogenation curves of $Li_{1.2}Na_{1.8}AlH_6$ obtained at temperatures of 443 K, 463 K, and 483 K, respectively; c) Isothermal hydrogenation curves of $Li_{1.3}Na_{1.7}AlH_6$ obtained at temperatures of 443 K, 463 K, and 483 K, respectively. The background hydrogen pressure was 5 MPa.

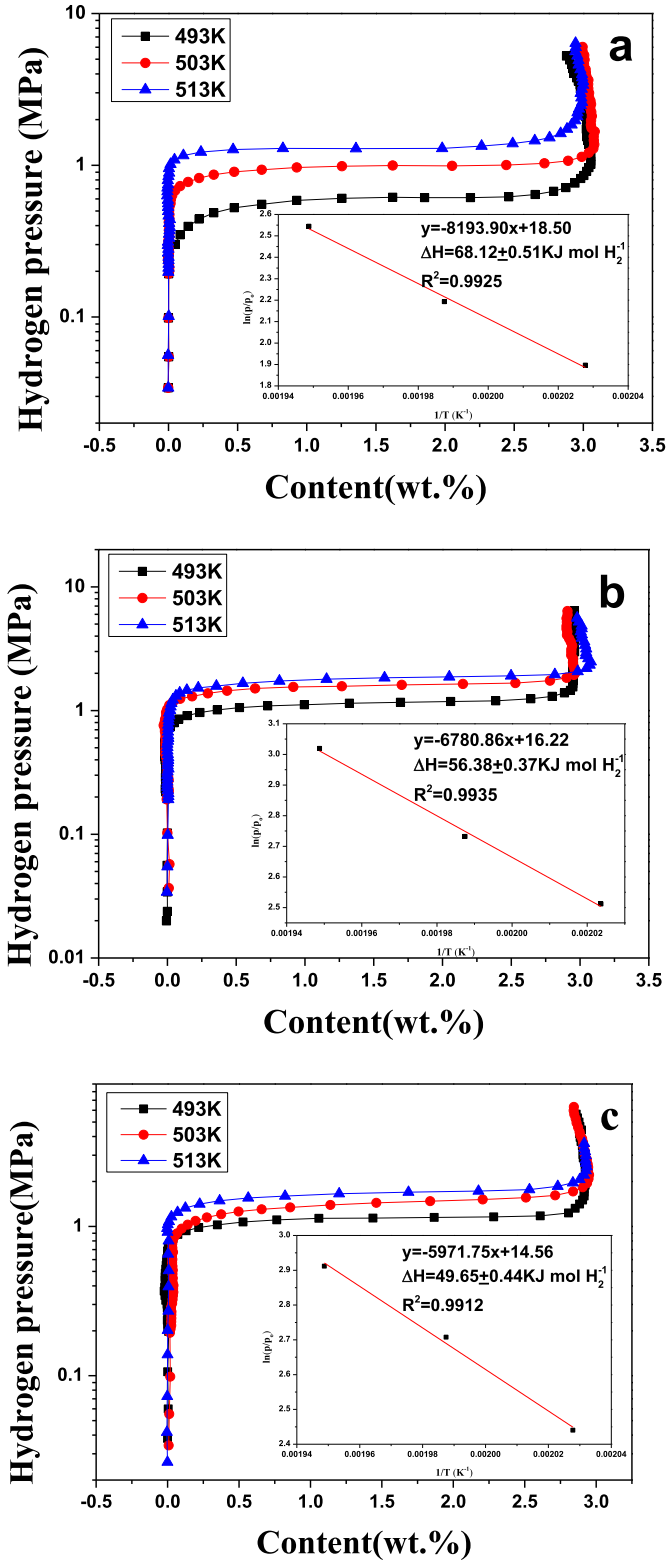

Fig. 8. a) PC isotherm curves of $LiNa_2AlH_6$ tested at 493 K, 503 K and 513 K, respectively; b) PC isotherm curves of $Li_{1.2}Na_{1.8}AlH_6$ tested at 493 K, 503 K and 513 K, respectively; c) PC isotherm curves of $Li_{1.3}Na_{1.7}AlH_6$ tested at 493 K, 503 K and 513 K, respectively. Their van't Hoff plots were exhibited in respective diagrams.

XRD analysis indicated that the formation range of $Li_xNa_{3-x}AlH_6$ compounds was x = 0.9–1.3 in composition.

Table 2
The dehydrogenation enthalpies of $Li_xNa_{3-x}AlH_6$ compounds.

Compound	$LiNa_2AlH_6$	$Li_{1.2}Na_{1.8}AlH_6$	$Li_{1.3}Na_{1.7}AlH_6$
ΔH(KJ mol^{-1} H_2^{-1})	68.1	56.4	49.7

2) The $Li_{1.3}Na_{1.7}AlH_6$ exhibited the best dehydrogenation performance among these Li-Na-Al-H compounds, of which the onset temperature was reduced by more than 40 K from other Li-Na-Al-H compounds.
3) The products of $Li_{1.3}Na_{1.7}AlH_6$ after dehydrogenation exhibit superior hydrogenation kinetics over the other Li-Na-Al-H compounds.
4) $Li_{1.3}Na_{1.7}AlH_6$ possesses the lowest thermal stability and activation energy for dehydrogenation among these Li-Na-Al-H compounds. Both thermodynamic and kinetic properties of $Li_{1.3}Na_{1.7}AlH_6$ synergistically improve its de/re-hydrogenation performances.

Acknowledgements

We are grateful for support from the National Natural Science Foundation of China (51571112, 51471087, and 11472080); the Natural Science Foundation of Jiangsu Province of China (BK20151405, 13KJA430003); Jiangsu Key Laboratory for Advanced Metallic Materials (BM2007204); The Six Talent Peaks Project in Jiangsu Province (2015-XNY-002); and the Fundamental Research Funds for the Central Universities (3212006402).

Appendix A. Supplementary data

Supplementary data related to this article can be found at https://doi.org/10.1016/j.jallcom.2017.09.205.

References

[1] L. Schlapbach, A. Züttel, Hydrogen-storage materials for mobile applications, Nature 414 (2001) 353–358.
[2] https://energy.gov/eere/fuelcells/downloads/doe-targets-onboard-hydrogen-storage-systems-light-duty-vehicles.
[3] B. Bogdanović, M. Schwickardi, Ti-doped alkali metal aluminium hydrides as potential novel reversible hydrogen storage materials, J. Alloys Compd. 253–254 (1997) 1–9.
[4] B. Bogdanović, M. Schwickardi, Ti-doped $NaAlH_4$ as a hydrogen-storage material – preparation by Ti-catalyzed hydrogenation of aluminum powder in conjunction with sodium hydride, J. Appl. Phys. A 72 (2001) 221–223.
[5] A. Zaluska, L. Zaluski, J.O. Ström-Olsen, Sodium alanates for reversible hydrogen storage, J. Alloys Compd. 298 (2000) 125–134.
[6] R.A. Zidan, S. Takara, A.G. Hee, C.M. Jesen, Hydrogen cycling behavior of zirconium and titanium–zirconium-doped sodium aluminum hydride, J. Alloys Compd. 285 (1999) 119–122.
[7] K.T. Møller, J.B. Grinderslev, T.R. Jensen, A $NaAlH_4$ -$Ca(BH_4)_2$, composite system for hydrogen storage, J. Alloys Compd. 720 (2017) 479–501.
[8] Y. Huang, P. Li, Q. Wan, J. Zhang, Y. Li, R. Li, X. Dong, X. Qu, Improved dehydrogenation performance of $NaAlH_4$ using $NiFe_2O_4$ nanoparticles, J. Alloys Compd. 709 (2017) 850–856.
[9] H. Cheng, Y. Chen, W. Sun, H. Lou, Y. Liu, Q. Qi, J. Zhang, J. Liu, K. Yan, H. Jin, Y. Zhang, S. Yang, The enhanced de/re-hydrogenation performance of $4MgH_2$ -$NaAlH_4$ composite by doping with TiH_2, J. Alloys Compd. 698 (2017) 1002–1008.
[10] J. Huang, M. Gao, Z. Li, X. Cheng, J. Gu, Y. Liu, H. Pan, Destabilization of combined $Ca(BH_4)_2$ and $Mg(AlH_4)_2$ for improved hydrogen storage properties, J. Alloys Compd. 670 (1) (2016) 135–143.
[11] C.H. Yang, T.T. Chen, W.T. Tsai, B.H. Liu, In situ, synchrotron X-ray diffraction study on the improved dehydrogenation performance of $NaAlH_4$–$Mg(AlH_4)_2$ mixture, J. Alloys Compd. 577 (45) (2013) 6–10.
[12] R. Wu, H. Du, Z. Wang, M. Gao, H. Pan, Y. Liu, Remarkably improved hydrogen storage properties of $NaAlH_4$, doped with 2D titanium carbide, J. Power Sources 327 (2016) 519–525.
[13] M. Paskevicius, U. Filsø, F. Karimi, J. Puszkiel, P. Pranzas, C. Pistidda, A. Hoell, E. Welter, A. Schreyer, T. Klassen, M. Dornheim, T.R. Jensen, Cyclic stability and structure of nanoconfined Ti-doped $NaAlH_4$, Int. J. Hydrogen Energy 41 (7) (2016) 4159–4167.

[14] Y. Liu, X. Zhang, K. Wang, Y. Yang, M. Gao, H. Pan, Achieving ambient temperature hydrogen storage in ultrafine nanocrystalline TiO_2@C-doped $NaAlH_4$, J. Mater. Chem. A 4 (2015) 1087–1095.
[15] C.M. Jensen, K.J. Gross, Development of catalytically enhanced sodium aluminum hydride as a hydrogen-storage material, J. Appl. Phys. A 72 (2001) 213–219.
[16] C.M. Jensen, R. Zidan, N. Mariels, A. Hee, C. Hagen, Advanced titanium doping of sodium aluminum hydride: segue to a practical hydrogen storage material, Int. J. Hydrogen Energy 24 (1999) 461–465.
[17] P. Claudy, B. Bonnetot, J.P. Bastide, J.M. Létoffé, Reactions of lithium and sodium aluminium hydride with sodium or lithium hydride. Preparation of a new alumino-hydride of lithium and sodium $LiNa_2AlH_6$, Mater. Res. Bull. 17 (1982) 1499–1504.
[18] O.M. Løvvik, O. Swang, Structure and stability of possible new alanates, J. Epl. 67 (2004) 607.
[19] O.M. Løvvik, O. Swang, S.M. Opalka, Modeling alkali alanates for hydrogen storage by density-functional band-structure calculations, J. Mater. Res. 20 (2005) 3199–3213.
[20] J. Huot, S. Boily, V. Güther, et al., Synthesis of Na_3AlH_6, and Na_2LiAlH_6, by mechanical alloying, J. Alloys Compd. 283 (1999) 304–306.
[21] Y. Liu, F. Wang, Y. Cao, M. Gao, H. Pan, Reversible hydrogenation/dehydrogenation performances of the Na_2LiAlH_6–$Mg(NH_2)_2$ system, Int. J. Hydrogen Energy 35 (2010) 8343–8349.
[22] A. Fossdal, H.W. Brinks, J.E. Fonneløp, B.C. Hauback, Pressure–composition isotherms and thermodynamic properties of TiF_3-enhanced Na_2LiAlH_6, J. Alloys Compd. 397 (2005) 135–139.
[23] R. Genma, N. Okada, T. Sobue, H.H. Uchida, Mechanically milled alanates as hydrogen storage materials, Int. J. Hydrogen Energy 31 (2006) 309–311.
[24] S.M. Opalka, O.M. Loevvik, H.W. Brinks, P.W. Saxe, B.C. Haoback, Integrated experimental—theoretical investigation of the Na—Li—Al—H system, Inorg. Chem. 46 (2007) 1401.
[25] J. Graetz, Y. Lee, J.J. Reilly, S. Park, T. Vogt, Structures and thermodynamics of the mixed alkali alanates, J. Phys. Rev. B 71 (2005), 184115.
[26] N. Okada, R. Genma, Y. Nishi, H.H. Uchida, RE-oxide doped alkaline hydrogen storage materials prepared by mechanical activation, J. Mater. Sci. 39 (2004) 5503–5506.
[27] R. Genma, H.H. Uchida, N. Okada, Y. Nishi, Hydrogen reactivity of Li-containing hydrogen storage materials, J. Alloys Compd. 356–357 (2003) 358–362.
[28] X.Z. Ma, E. Martinez-Franco, M. Dornheim, T. Klassen, R. Bormann, Catalyzed Na_2LiAlH_6 for hydrogen storage, J. Alloys Compd. 404 (2005) 771–774.
[29] Y. Nakamura, A. Fossdal, H.W. Brinks, B.C. Hauback, Characterization of Al–Ti phases in cycled TiF_3-enhanced Na_2LiAlH_6, J. Alloys Compd. 416 (2006) 274–278.
[30] X. Fan, X. Xiao, L. Chen, S. Li, H. Ge, Q. Wang, Direct synthesis and hydrogen storage behaviors of nanocrystalline Na_2LiAlH_6, J. Mater. Sci. 46 (2011) 3314–3318.
[31] F. Wang, Y. Liu, M. Gao, K. Luo, H. Pan, Q. Wang, Formation reactions and the thermodynamics and kinetics of dehydrogenation reaction of mixed alanate Na_2LiAlH_6, J. Phys. Chem. C 113 (2009) 7978–7984.
[32] Y. Liu, F. Wang, Y. Cao, M. Gao, H. Pan, Q. Wang, Mechanisms for the enhanced hydrogen desorption performance of the TiF_4-catalyzed Na_2LiAlH_6 used for hydrogen storage, J. Energy Environ. Sci. 3 (2010) 645–653.
[33] L. Zaluski, A. Zaluska, J.O. Ström-Olsen, Hydrogenation properties of complex alkali metal hydrides fabricated by mechano-chemical synthesis, J. Alloys Compd. 290 (1999) 71–78.
[34] R. Santhanam, G.S. Mcgrady, Synthesis of alkali metal hexahydroaluminate complexes using dimethyl ether as a reaction medium, Inorg. Chim. Acta 361 (2008) 473–478.
[35] H.H. Cheng, W.B. Li, W. Chen, D.M. Chen, M.T. Wang, K. Yang, Development of hydrogen absorption–desorption experimental test bench for hydrogen storage material, Int. J. Hydrogen Energy 39 (2014) 13596–13602.
[36] A. Zaluska, L. Zaluski, J.O. Strom-Olsen, ChemInform abstract: structure, catalysis and atomic reactions on the nano-scale: a systematic approach to metal hydrides for hydrogen storage, Appl. Phys. A 32 (2001) 157–165.
[37] M.Y. Song, S.N. Kwon, H.R. Park, D.R. Mumm, Characterization of a magnesium-based alloy after hydriding-dehydriding cycling (n=1–150), Met. Mater. Int. 19 (2013) 1139–1144.
[38] J.R. Ares, K.F. Aguey-Zinsou, M. Porcu, J.M. Sykes, M. Dornheim, T. Klassen, R. Bormann, Thermal and mechanically activated decomposition of $LiAlH_4$, Mater. Res. Bull. 43 (5) (2008) 1263–1275.